Biosensors and Bioelectronics 26 (2011) 4111–4116

Contents lists available at ScienceDirect

Biosensors and Bioelectronics

journal homepage: www.elsevier.com/locate/bios

A "turn-on" fluorescent copper biosensor based on DNA cleavage-dependent graphene-quenched DNAzyme

Meng Liu, Huimin Zhao*, Shuo Chen, Hongtao Yu, Yaobin Zhang, Xie Quan*

Key Laboratory of Industrial Ecology and Environmental Engineering (Ministry of Education, China), School of Environmental Science and Technology, Dalian University of Technology, Dalian 116024, China

ARTICLE INFO

Article history:
Received 28 January 2011
Received in revised form 3 April 2011
Accepted 5 April 2011
Available online 12 April 2011

Keywords:
Biosensor
DNAzyme
DNA cleavage
Fluorescence
Graphene

ABSTRACT

A novel and promising "turn-on" fluorescent Cu^{2+} biosensor is designed based on graphene–DNAzyme catalytic beacon. Due to the essential surface and quenching properties of two-dimensional graphene, it can function as both "scaffold" and "quencher" of the Cu^{2+}-dependent DNAzyme, facilitating the formation of self-assembled graphene-quenched DNAzyme complex. However, Cu^{2+}-induced catalytic reaction disturbs the graphene–DNAzyme conformation, which will produce internal DNA cleavage-dependent effect. In this case, the quenched fluorescence in graphene–DNAzyme is quickly recovered to a large extent in 15 min. Compared with common DNAzyme-based sensors, the presented graphene-based catalytic beacon greatly improves the signal-to-background ratio, hence increasing the sensitivity (LOD = 0.365 nM). Furthermore, the controllable DNA cleavage reaction provides an original and alternative internal method to regulate the interaction between graphene and DNA relative to the previous external sequence-specific hybridization-dependent regulation, which will open new opportunities for nucleic studies and sensing applications in the future.

1. Introduction

In recent years, considerable efforts have been devoted to the detection of heavy-metal ions in both the aquatic environment and biological system due to their deleterious effects on public health and ecosystem. Of particular interest is the quantitative analysis of aqueous copper (Cu^{2+} or Cu^{+}). As one of the most important micronutrient elements for human life, low-level copper is essential for biological activities such as enzyme regulation, metabolism and immune function. However, it has been demonstrated that high-level copper exposure can lead to neural disturbance, liver or kidney damage (Georgopoulos et al., 2001; Zietz et al., 2003), as well as serious neurodegenerative diseases (Brown and Kozlowski, 2004; Vulpe et al., 1993; Waggoner et al., 1999), including Menkes and Wilson diseases, hereditary aceruloplasminemia, Alzheimer's disease, and prion diseases. In this regard, it is highly desirable to develop a facile, environment-friendly and high-throughout method for the determination of trace copper with high sensitivity and selectivity to meet the requirements in the fields of environmental monitoring, waste management and biology toxicology. Current protocols for the detection of copper generally require complex laboratory instruments, such as atomic absorption spectroscopy, inductively coupled plasma-mass spectrometry, and atomic fluorescence (FL) spectrometry, which realize their excellent performances at the expense of time and elaborate sample preparation or preconcentration processes. In response to these limitations, the past years witnessed great progress in the development of various optical probes for rapid, low-cost and practical detection of copper, such as fluorescent sensors based on organic fluorophores or chromogens (Wen et al., 2006; Zeng et al., 2006), novel-metal nanoclusters (Chen et al., 2009a; Shang and Dong, 2008), luminescent quantum dots or nanorods (Chan et al., 2010; Liu et al., 2010a), luminescent metal-organic framework (Chen et al., 2009b), and colorimetric sensors relied on Au nanoparticles (Xu et al., 2010; Zhou et al., 2008) or catalytic carbon nanotube (Song et al., 2010). Nevertheless, most of these strategies still suffer from either limitations with respect to selectivity, water solubility and stability or potential toxicity.

Ever since the discovery of DNAzyme (Breaker and Joyce, 1994), great interest has focused on the identification and filtration of the catalytic DNA via in vitro selection process, which exhibits catalytic activity or binding activity in the presence of specific cofactors including inorganic, organic and biomolecules, and even cells or viruses (Breaker, 1997; Carmi et al., 1996; Li et al., 2000; Li and Lu, 2000; Mei et al., 2003). As noted, the binding affinity of DNAzyme was demonstrated to rival protein antibody in terms of specific target molecules. In addition, the cofactor-dependent DNAzymes toward inorganic metal ions make them ideal recognition platforms in sensing resulting from their unique advantages over antibodies,

* Corresponding authors. Tel.: +86 411 84706263; fax: +86 411 84706263.
E-mail addresses: zhaohuim@dlut.edu.cn (H. Zhao), quanxie@dlut.edu.cn (X. Quan).

0956-5663/$ – see front matter © 2011 Elsevier B.V. All rights reserved.
doi:10.1016/j.bios.2011.04.006

such as facile preparation and outstanding stability under harsh conditions. Therefore, many novel principles based on DNAzyme have been designed to detect Cu^{2+} (Liu and Lu, 2007a, 2007b; Qin et al., 2010a; Wu et al., 2010; Yin et al., 2009), Pb^{2+} (Liu and Lu, 2003, 2005; Li et al., 2010a; Wang et al., 2008), Hg^{2+} (Liu and Lu, 2007c; Li et al., 2009), UO_2^{2+} (Lee et al., 2008; Moshe et al., 2009), and K^+ (Kong et al., 2009; Li et al., 2010b, 2010c; Qin et al., 2010b) with high sensitivity and selectivity, producing fluorescent, electrochemical as well as colorimetric outputs. Among them, fluorescent sensors particularly allow a powerful signal for practical on-site and real-time detection with portable fluorimeters. For example, in a typical Cu^{2+}-dependent DNAzyme sensor (Liu and Lu, 2007a), the fluorophore-labeled substrate strand quenched by a quencher-modified enzyme through energy or electron transfer will irreversibly be cleaved and then released to recover the FL signal in the presence of the target. In this case, it is a big challenge in the design of labeling components and strategies capable of reducing the background signal. In general, most current functional DNAzyme-based sensors require the covalent attachment of two or more quenchers to either the end or the internal site of one DNA strand (Liu and Lu, 2007a; Mei et al., 2003), which will inevitably lead to not only a complicated or expensive operation, but also a weaker performance of DNAzyme in comparison with their label-free analogues. Alternatively, efforts have been made to develop DNAzyme-based label-free fluorescent sensors relied on binding-dependent FL activation and dynamic cleavage activity (Xiang et al., 2009, 2010; Xu and Lu, 2010). Despite of the progress, there is still need to explore other general platforms in label-free sensors that could further improve the signal-to-background ratio, strengthen the binding affinity of organic dyes to DNAzyme, and avoid the introduction of dSpacer into adenosine aptamers (Xiang et al., 2009). Therefore, it is necessary and urgent to search for universal signaling strategies and introduce novel materials to break these limitations in traditional DNAzyme-based sensors.

With the tremendous progress in nanotechnology, low-dimensional nanomaterials have emerged as efficient "scaffold" and "quencher" of biomolecules due to their unique surface and electronic properties (Kata and Willner, 2004; Wang et al., 2009). In particular, two-dimensional graphene-based material has shown great potential as novel platform in constructing DNA biosensor by means of strong π-stacking interactions between the nucleotide bases in single-stranded DNA and the graphene surface (Dong et al., 2010; He et al., 2010; Lu et al., 2009; Tang et al., 2010). Besides, graphene-based material can act as highly efficient super-quencher of the fluorophore based on both electron transfer and energy transfer processes, providing a powerful basis for fluorescent sensors. In our previous study, we demonstrated that nano-scale graphene sheet can obscure the traditional donor-to-acceptor distance in a self-assembled fluoroimmunoassay (Liu et al., 2010b). In other words, the effective graphene-biomolecule configurations were independent on the size or orientation of donors to a large extent, producing a distance-independent quenching effect. Therefore, taking advantage of the remarkable interaction between two-dimensional graphene and DNA bases, as well as the essential distance-independent quenching effect of graphene, it is possible to explore self-assembled graphene–DNAzyme complex in designing a facile, rapid and sensitive platform for the detection of heavy metal ions. In this study, we presented a general method for "turn-on" DNAzyme catalytic beacon for Cu^{2+} ions by employing fluorophore-labeled Cu^{2+}-dependent DNAzyme as recognition site and two-dimensional graphene as the FL transduction unit. The key factor was an internal controllable competition that allowed the cleaved DNA liberating from the graphene surface, which provided a vigorous basis for our design. Compared with conventional DNAzyme-based sensors, this novel self-assembled catalytic beacon required only one end labeled fluorophore, which maintained the high catalytic activity of DNAzyme. Furthermore, it improved the signal-to-background ratio due to the exceptional DNA-binding selectivity of graphene. More importantly, we demonstrated that the graphene–DNA interaction could also be readily tuned by the dynamic cleavage of DNA relative to external sequence-specific hybridization-dependent graphene–DNA interaction in common graphene-based sensing platform, thus opening new opportunities for the design and engineering of graphene–DNA complex-based applications.

2. Materials and methods

2.1. Materials and reagents

The nucleic acids Cu-Sub (5′-T_{10}AGCTTCTTTCTAATACGGCTT-ACC-FAM-3′) and Cu-Enz (5′-GGTAAGCCTGGGCCTCTTTCTTTTTAA-GAAAGAAC-3′) were purchased from Takara Biotechnology Co. (Dalian, China) and purified by high-performance liquid chromatography (HPLC). $KMnO_4$, NaCl, $CdCl_2$, $CuCl_2$, $Pb(NO_3)_2$, $ZnCl_2$, $CaCl_2$, $FeCl_3$, $MnCl_2$, $BaCl_2$ and $CoCl_2$ were of analytical reagent grade and purchased from the Kemiou Agent Co., Tianjin, China. Sodium ascorbate was obtained from Sinopharm Chemical Reagent Co., Ltd (China). Other reagents such as NaOH, HCl, HNO_3, H_2O_2 (30%), acetone and anhydrous ethanol were used as received without any further treatment. Ultrapure water obtained from a Millipore water purification system (resistivity >18.0 MΩ cm^{-1}, Laikie Instrument Co., Ltd., Shanghai, China) was used throughout. All the glassware was first cleaned with a mixture of HCl and HNO_3 (ratio of HCl/HNO_3 = 3:1 in volume) and thoroughly rinsed with ultrapure water. Phosphate buffer solution (PBS, 0.05 M) with various pH values was prepared by mixing the stock solution of Na_2HPO_4 and NaH_2PO_4 with different volume ratios.

2.2. Instruments

Atomic force microscopy (AFM) measurements were carried out on Agilent PicoPlus II. The AFM sample was prepared by casting 5 μL of graphene dispersion on a freshly-cleaved mica surface. FL measurements were performed using Hitachi F-4500 fluorescence spectrometer with a scan rate at 1200 nm/min. The excitation wavelength was set at 494 nm, and the photomultiplier tube (PMT) voltage was 700 V. The slits for excitation and emission were set at 5 nm/10 nm. The FT-IR measurements on powdered samples were made using a Bruker VERTEX 70 Fourier Transform Infrared Spectrometer in transmission mode with a KBr window. The Raman spectra were obtained by a Renishaw Micro-Raman System 2000 Spectrometer operated at He–Ne laser excitation (wavelength 623.8 nm; laser power 35 mW) with a beam spot size of about 2 μm.

2.3. Preparation of graphene oxide and graphene sheet

Graphene oxides (GO) were prepared by our previously reported method (Liu et al., 2010b). Briefly, graphite powder (1.0 g) was first dispersed in concentrated H_2SO_4 (23 mL) at room temperature. $KMnO_4$ (3 g) was then added gradually under stirring at 0 °C. Successively, the mixture was sonicated for 6 h to give a dark green solution. Afterward, ultrapure water (46 mL) was slowly transferred to the mixture. After keeping boiling for 30 min, the reaction was then terminated by adding ultrapure water (140 mL) and H_2O_2 solution (30%, 10 mL). Finally, the resultant yellow product was separated by centrifugation, and washed with 5% HCl solution and ultrapure water, sequently. An environment-friendly hydrothermal route was employed to convert graphene oxide to graphene (Zhou et al., 2009). The obtained graphene sheet could be readily dispersed in water due to the residually carboxylic acid groups at

the edges (Li et al., 2008; Liu et al., 2008). The resultant aqueous dispersion of graphene (0.12 mg/mL) was stored at room temperature and employed in the following work.

2.4. Preparation of DNAzyme

To form the Cu^{2+}-dependent DNAzyme, 2 μM Cu-Sub and 2 μM Cu-Enz were annealed in a buffer containing 50 mM PBS, 0.5 M NaCl, pH 7.0. The mixture was warmed to 95 °C for 1 min in a water bath and subsequently allowed to cool naturally to room temperature. The resultant DNAzymes were stored in a 4 °C dark room.

2.5. FL assay of Cu^{2+}

In a typical experiment, 380 μL of buffer (50 mM PBS, 50 mM NaCl, pH 7.4), 10 μL of DNAzyme, 20 μL of sodium ascorbate (5 mM) and 80 μL of graphene solution (0.12 mg/mL) were sequentially added into a microcentrifuge tube. After 30 min reaction, the solution was transferred to a quartz cell at room temperature. Subsequently, 10 μL of Cu^{2+} stock solution was added to the mixture for time-dependent FL measurement at $\lambda_{ex}/\lambda_{em}$ = 494/518 nm.

2.6. Electrophoresis analysis

Cu^{2+}-dependent DNAzymes before and after the catalytic reaction were respectively loaded onto 6× loading buffer containing 30 mM EDTA, 36% (v/v) Glycerol, 0.05% (w/v) Xylene Cyanol FF, and 0.05% (w/v) Bromophenol blue, pH 7.0. The samples were then put on a 20% polyacrylamide gel in a 1× TAE buffer (40 mM Tris acetate, 2 mM EDTA, pH 8.5) followed by electrophoresis for 180 min at 60 V to separate cleaved DNA. After ethidium bromide staining, the gel was imaged using a G: BOX HR system (Gene Co., Ltd.).

2.7. Analysis of drinking water samples

A series of testing samples were prepared by mixing drinking water with standard Cu^{2+} solution. The samples (10 μL) were then added to graphene–DNAzyme solution (total volume, 500 μL) containing 50 mM PBS (pH 7.4), 50 mM NaCl, 0.2 mM sodium ascorbate and 19.2 μg/mL graphene. Subsequently, time-dependent FL measurements were recorded at $\lambda_{ex}/\lambda_{em}$ = 494/518 nm.

3. Results and discussion

3.1. Design strategy

An ideal DNAzyme catalytic beacon should provide a low FL background by employing effective quenchers, further enabling the prompt separation of the cleaved substrate during the cleavage reaction. In order to achieve the above sensing performance, we designed a novel catalytic beacon for Cu^{2+} as shown in Fig. 1. The system was a combination of two components that formed a self-assembled complex. The first component was the Cu^{2+}-dependent DNAzyme containing a 3′-FAM-modified Cu-Sub and a Cu-Enz, which served as an effective recognition site. As noted, there was no additional labeled quencher in the DNAzyme. The second component was the FL transduction unit of graphene, which was employed as an independent quencher to suppress background signal. Initially, despite of the DNAzyme containing engineered duplex and triplex regions or structures, optimum amount of graphene guaranteed the fluorophore in close proximity to the graphene surface, facilitating the following complete quenching. In the presence of Cu^{2+}, the DNA substrate was irreversibly cleaved as a result of the specific DNAzyme–Cu^{2+} interaction, thus disturbing the self-assembled graphene–DNAzyme conformation. In such a case, the "released" FAM-labeled DNA strand in turn produced

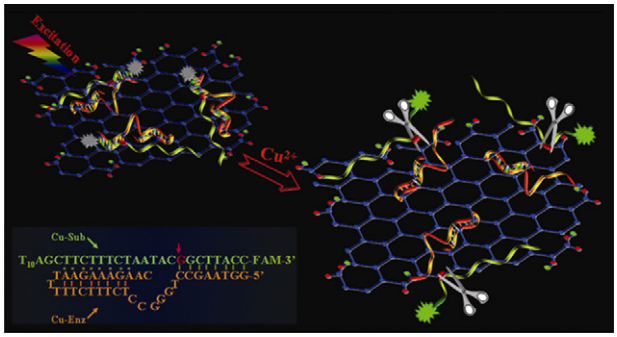

Fig. 1. Schematic illustration of "turn-on" fluorescent Cu^{2+} sensor based on DNA cleavage-dependent self-assembled graphene-quenched DNAzyme.

a concentration-dependent FL signal. Compared with the normal DNAzyme-based designs, it was apparent that this strategy provided a robust and cost-effective construction by utilizing both the intrinsic advantage of two-dimensional graphene and catalytic DNA.

3.2. Characterization of graphene sheet

AFM was employed to characterize the morphology and thickness of a graphene sheet. A typical AFM image showed a high-quality single-layer graphene sheet with the lateral width of hundreds nanometers and the relatively low amount of defects or disorders (Fig. S1A In Supplementary Material). The cross-section of a AFM image indicated that the resultant graphene sheet was with an average height of 10 Å (Fig. S1B), which was consistent with the single-layer graphene of 0.8–1.2 nm reported by other groups (Cote et al., 2009; Guo et al., 2009; Kim et al., 2010).

The FT-IR spectroscopy and Raman spectrum further provided the information of graphene. As shown in Fig. S1C, functional groups of GO were observed in FT-IR spectrum, which displayed the presence of O–H (3400 cm^{-1}), C=O (1733 cm^{-1}), C=C (1625 cm^{-1}), and C–O (1070 cm^{-1}). After hydrothermal reduction, most oxygen-containing groups decreased dramatically and even disappeared entirely. In addition, two typical peaks at 1340 and 1590 cm^{-1} appeared (Fig. S1D), which could be assigned to the D-band (the symmetry A_{1g} mode) and G-band (the E_{2g} mode of sp^2 carbon atoms) in graphene, respectively. Taken together, these results suggested that GO were successfully reduced into graphene by a simple hydrothermal dehydration route.

3.3. DNA cleavage-dependent graphene–DNA interaction

Earlier studies demonstrated that graphene-based material possessed different adsorption affinity for single-stranded DNA (ssDNA) and double-stranded DNA (dsDNA) (He et al., 2010; Lu et al., 2009), which led to the differences in quenching efficiency and FL signals. Interestingly, we observed that the FL of FAM-modified DNAzyme was effectively quenched by graphene as well, although the DNAzyme was composed of engineered duplex and triplex elements. Fig. 2A showed the FL emission spectra of DNAzyme under different conditions. Upon excitation at 494 nm, FAM-labeled DNAzyme remained strong FL intensity in PBS buffer solution. As expected, over 99% FL was quenched with the presence of 19.2 μg/mL of graphene, suggesting the formation of self-assembled graphene–DNAzyme complex (Lu et al., 2009), which then brought the FAM and the graphene surface in close proximity. As shown in Fig. 2B, both the quenching kinetics rate and the quenching efficiency were depended on the concentration of graphene. Furthermore, the quenching reaction reached equilibrium only in several minutes, indicating the high self-assembled

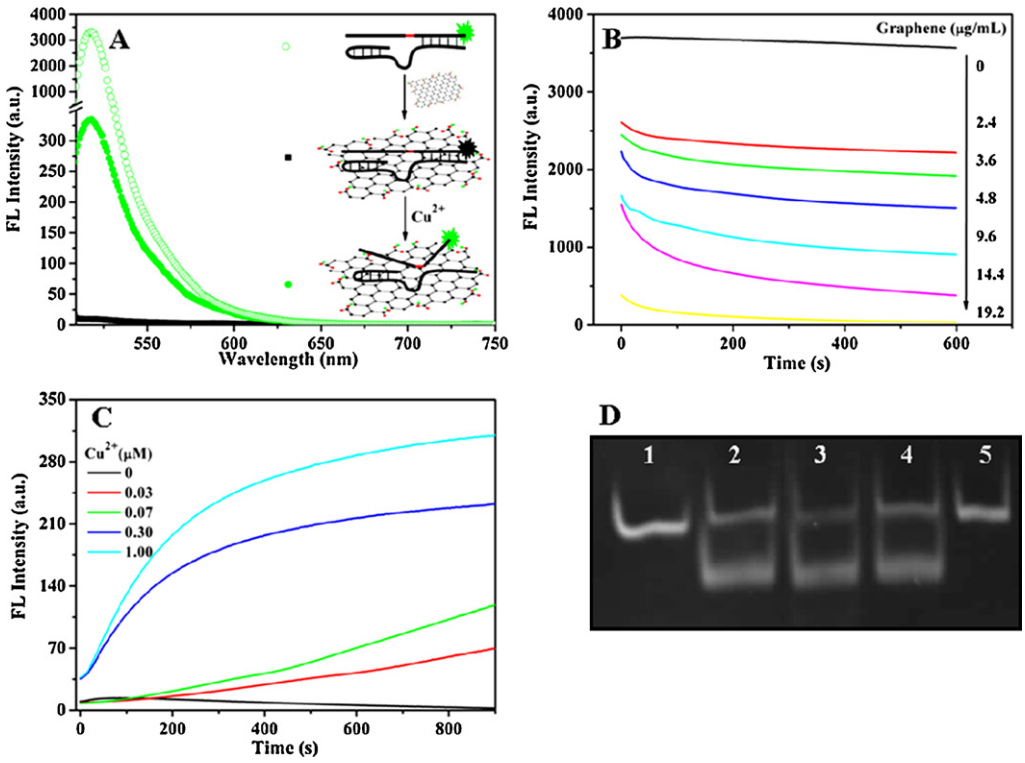

Fig. 2. (A) Steady-state FL spectra of DNAzyme at different conditions. (B) Kinetics study for FL changes of the DNAzyme with different concentrations of graphene. (C) Kinetics study for FL changes of the graphene-quenched DNAzyme in the presence of various amounts of Cu^{2+}. The concentrations of Cu-Sub and Cu-Enz were 40 nM and 40 nM, respectively. The buffer contained 50 mM PBS (pH 7.4), 50 mM NaCl, 0.2 mM sodium ascorbate and 19.2 μg/mL graphene. $\lambda_{ex}/\lambda_{em}$ = 494/518 nm. (D) Gel-electrophoresis image of the DNAzyme. Lane 1 contained 1 μM DNAzyme; Lanes 2–4 were the DNAzyme incubated for 5, 10, 15 min after the addition of 25 μM Cu^{2+}. Lane 5 was the Cu-Sub with Cu^{2+}.

rate of the DNAzyme on graphene. To demonstrate the potential use of self-assembled graphene-quenched Cu^{2+}-dependent DNAzyme in the detection of Cu^{2+}, FL response was investigated in the presence of the target. Fig. 2C showed the kinetics of FL enhancement as a function of reaction time, displaying an increasing rate with higher concentrations of Cu^{2+}. Moreover, a 32-fold FL enhancement comparable to the original intensity was observed when the concentration of Cu^{2+} reached 1 μM, probably due to the Cu^{2+}-induced catalytic cleavage of DNAzyme and the following release of FAM-labeled DNA strands. As noted, the enhancement is much higher than the 13-fold enhancement of the catalytic beacon with dual quenchers (Liu and Lu, 2007a), demonstrating that graphene-quenched DNAzyme approach could potentially improve the sensitivity in the catalytic beacon for Cu^{2+} determination.

It was well-known that both zero-dimensional Au nanoparticles (NPs) (Jennings et al., 2006; Singh and Strouse, 2010; Yun et al., 2005) and one-dimensional carbon nanotubes (Liu et al., 2009; Yang et al., 2008a, 2008b; Zhang et al., 2010a) were successfully applied as excellent FL acceptors or quenchers for organic fluorophore or inorganic luminescent nanomaterial in fluorescent assay. Furthermore, the differences in the adsorption properties of either Au NPs or carbon nanotubes toward ssDNA and dsDNA offered the basis for their applications in molecular beacon and DNA sensing (Jeng et al., 2006; Yang et al., 2008b). At this point, the performance of the two-dimensional graphene-based material was similar to that of Au NPs or carbon nanotubes. Nevertheless, it was observed that the interaction between Au NPs and DNA was inherently dependent on the dipole orientation of zero-dimensional Au NPs as well as the DNA configuration (Kim et al., 2006; Saini et al., 2009). As a result, further development of Au NPs-based assay was hampered by its dependence on donor-acceptor distance, beyond which the transfer rate and quenching efficiency were dramatically reduced. The quenching behavior of one-dimensional carbon nanotube and graphene were also compared as follows. In general, the adsorption rate of DNA on the surface of carbon nanotube was slow at room temperature (Yang et al., 2008a, 2008b). Therefore, a best quenching efficiency was obtained almost in 1 h (Yang et al., 2008a), hindering its further application as a general platform. Moreover, due to the one-dimensional surface effect of the carbon nanotube, the interaction between DNA (especially for hairpin-structured DNA) and carbon nanotube was dependent on the DNA configuration (Yang et al., 2008b), hence limiting the quenching behavior as well as the quenching efficiency in the self-assembled carbon nanotube-DNA complex. In direct contrast, the graphene-based material not only provided better quenching behavior but also improved the sensing performance, which resulted from its distance-independent quenching effect and two-dimensional surface effect (Liu et al., 2010b; Lu et al., 2009).

To confirm that the above FL changes of DNAzyme were due to the Cu^{2+}-catalyzed cleavage reaction, gel-electrophoresis was carried out to measure the activity of 1 μM DNAzyme in the presence of 25 μM Cu^{2+}. As shown in Fig. 2D, DNA bands were well-separated after the addition of Cu^{2+}, indicating the effective cleavage reaction (Liu and Lu, 2007a). Considering the interaction between graphene and DNA, it could be concluded that a two-step process, including DNA cleavage and graphene/DNA adsorption, happened in the presence of the target. In principle, the FL of cleaved DNA should be quenched completely due to the π-stacking interaction between graphene and DNA (Dong et al., 2010; He et al., 2010; Lu et al., 2009; Tang et al., 2010). While in reality, the quenched FL in graphene–DNAzyme was quickly recovered to a large extent in 15 min, implying that cleaved DNA was liberated from the graphene surface during the catalytic reaction. Therefore, we drew a conclusion that the DNA cleavage rate was significantly higher than the binding rate of DNA strand with graphene, resulting in the released FAM-modified DNA. We believed that the surface effect of graphene

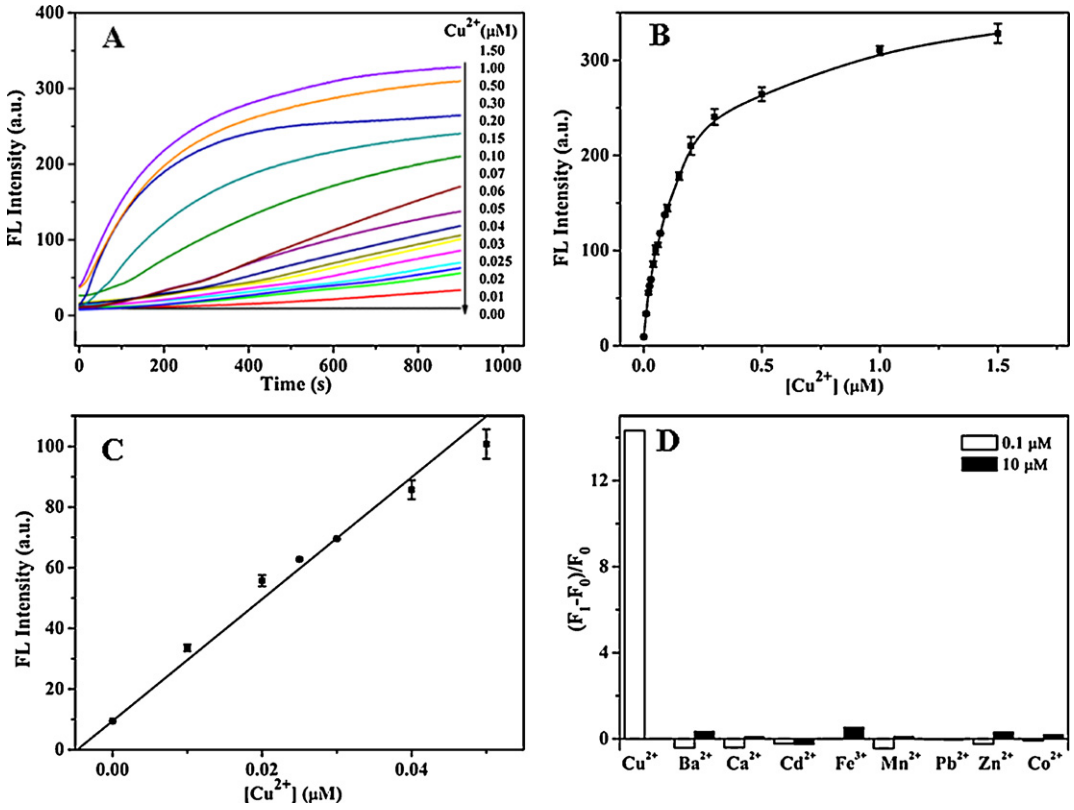

Fig. 3. (A) Kinetics of FL enhancement with varying concentrations of Cu^{2+}. (B) FL enhancement as a function of Cu^{2+} concentration (0–1.5 μM). (C) The linear responses at low concentrations (0–0.05 μM). (D) Selectivity of our sensor for Cu^{2+} detection over other metal ions. The concentration of Cu^{2+} was set at 0.1 μM. Error bars represented standard deviations from three repeated measurements. The concentrations of Cu-Sub and Cu-Enz were 40 nM and 40 nM, respectively. The buffer contained 50 mM PBS (pH 7.4), 50 mM NaCl, 0.2 mM sodium ascorbate and 19.2 μg/mL graphene. $\lambda_{ex}/\lambda_{em}$ = 494/518 nm.

and DNA cleavage-dependent effect contributed to the basis of our proposed design. Remarkably, this DNA-cleavage-dependent effect in self-assembled graphene–DNA complex provided an internal method to regulate the interaction between graphene and DNA. In comparison with the external competition-dependent effect in previously reported graphene–DNA-based platform (Dong et al., 2010; He et al., 2010; Lu et al., 2009; Tang et al., 2010), the alternative and controllable internal competition-dependent effect in graphene–DNA complex was expected to extend its applications (especially for the situation not suitable to pose an external competition) in the future.

3.4. Sensor optimization

We employed signal-to-background ratio (S/B) to reflect the sensing performance in different systems (Liu et al., 2009; Yang et al., 2008a). The S/B was defined as $(F_1 - F_{buffer})/(F_0 - F_{buffer})$, where F_1, F_0, and F_{buffer} were the FL intensities of the probe-target hybrid, probe without target and buffer solution, respectively. The ratio between Cu-Sub and Cu-Enz in DNAzyme was first optimized to obtain the best sensing performance. As shown in Fig. S2A (In Supplementary Material), a decrease of the ratio of Cu-Enz in DNAzyme (ratios 2:1, 3:2 and 1:1) resulted in a gradual decrease of background signal, and an increase of S/B, implying that optimal ratio of Cu-Enz could facilitate the interaction of the DNAzyme with graphene. For example, a S/B as high as 21.2 was obtained with the 1:1 Cu-Enz to Cu-Sub ratio. However, further reducing the Cu-Enz affected the DNAzyme performance, resulting in slow catalytic kinetics and decreased S/B (Fig. S2B).

pH was also one of the most important parameters in the catalytic reaction. As shown in Fig. S3A (In Supplementary Material), the kinetics rates of FL enhancement increased when the pH ranged from 6.0 to 7.4, and then decreased when pH further increased to 8.0, in accordance with the trends of S/B (Fig. S3C). It was reported that DNAzyme-based biosensors were effective in neutral pH (Xiang et al., 2009, 2010; Zhang et al., 2010b). In addition, it was well-known that FL intensity of FAM increased with the increasing pH (Fig. S3B). Consequently, we attributed the FL enhancement at pH 7.4 to the effect of pH-dependent FAM. The concentration of salt was another key factor in optimal sensor due to its effects on the catalytic activity of DNAzyme and the stability of graphene (Fig. S4A). As shown in Fig. S4B (In Supplementary Material), the S/B increased to 19.7 with the salt concentration increasing from 0 mM to 50 mM, and then decreased to 11.75 when the salt concentration was up to 100 mM. On the basis of these results, a Cu^{2+}-dependent DNAzyme with the 1:1 Cu-Enz to Cu-Sub ratio in a pH 7.4 PBS buffer solution containing 50 mM NaCl was selected for the following experiments.

3.5. Sensor performance

Under the optimal condition, the sensitivity and selectivity of the sensor were investigated, respectively. A kinetics study was carried out to record the time-dependent FL changes at 518 nm after the addition of various amounts of Cu^{2+}. As shown in Fig. 3A, the FL intensity gradually increased with the reaction time. Furthermore, the kinetics of FL enhancement was indeed dependent on the concentration of Cu^{2+}. Fig. 3B presented the calibration curve of the sensor in the range from 0.01 to 1.5 μM. For the control experiment, no FL enhancement was observed in the absence of the target. The detection limit was determined to be 0.365 nM on the basis of the 3σ/slope (Fig. 3C), which was much lower than that of previously

reported DNAzyme-based copper sensor (Liu and Lu, 2007a, 2007b; Qin et al., 2010a; Wu et al., 2010; Yin et al., 2009), and at least 95 times lower compared to that of dual quenchers labeled sensors (Liu and Lu, 2007a). We believed that the excellent quenching behavior of graphene and DNA cleavage-dependent effect were the main contributors to the better sensitivity.

To understand the selectivity of the system, we measured its response in the environmentally relevant ionic species including Ba^{2+}, Ca^{2+}, Cd^{2+}, Fe^{3+}, Mn^{2+}, Pb^{2+}, Zn^{2+}, Co^{2+} with the concentrations of 0.1 μM and 10 μM (Fig. 3D). The results revealed that the competitive metal ions yielded only minimal responses even at relatively high concentration levels, indicating that this method had good selectivity, which was comparable with the selectivity of the original Cu^{2+}-dependent DNAzyme sensor.

3.6. Sensor application

To explore the practicality of the present approach, the designed self-assembled graphene–DNAzyme complex was used to analyze Cu^{2+} in drinking water. We first obtained a linear correlation ($R = 0.997$) between the FL response and the concentration of Cu^{2+} in the drinking water (Fig. S5, In Supplementary Material). Then two prepared samples with as-known concentration were tested to evaluate the feasibility of the approach (Fig. S6). As shown in Table S1 (In Supplementary Material), the self-assembled graphene–DNAzyme catalytic beacon provided recoveries of 94.3–103%, suggesting that our graphene-quenched DNAzyme system was successful in detection of Cu^{2+} in environmental samples.

4. Conclusions

In conclusion, we designed a promising self-assembled graphene–DNAzyme catalytic beacon for Cu^{2+} based on internal DNA cleavage-dependent graphene–DNA interaction. Due to the intrinsic advantage of two-dimensional graphene and the catalytic activity of Cu^{2+}-dependent DNAzyme, the novel catalytic beacon not only provided convenient protocol but also effectively increased the sensitivity in environmental monitoring. Future experiments that further improve the sensitivity are being conducted. Moreover, the internal and controllable competition between graphene and DNA was presented, which will open new opportunities for the development of extended system in molecular engineering and biosensor design.

Acknowledgments

This work was supported by the National Basic Research Program of China (2011CB936002), National Natural Science Foundation of China (No. 20877012), the Program for New Century Excellent Talents in University (NCET-08-0079), the Fundamental Research Funds for the Central Universities (DUT 10ZD115) and Program for Changjiang Scholars and Innovative Research Team in University (IRT0813).

Appendix A. Supplementary data

Supplementary data associated with this article can be found, in the online version, at doi:10.1016/j.bios.2011.04.006.

References

Breaker, R.R., 1997. Nat. Biotechnol. 15, 227–231.
Breaker, R.R., Joyce, G.F., 1994. Chem. Biol. 1, 223–229.
Brown, D.R., Kozlowski, H., 2004. Dalton Trans., 1907–1917.
Carmi, N., Shultz, L.A., Breaker, R.R., 1996. Chem. Biol. 3, 1039–1046.
Chan, Y.-H., Chen, J.X., Liu, Q.S., Wark, S.E., Son, D.H., Batteas, J.D., 2010. Anal. Chem. 82, 3671–3678.
Chen, W.B., Tu, X.J., Guo, X.Q., 2009a. Chem. Commun., 1736–1738.
Chen, B.L., Wang, L.B., Xiao, Y.Q., Fronczek, F.R., Xue, M., Cui, Y.J., Qian, G.D., 2009b. Angew. Chem. Int. Ed. 48, 500–503.
Cote, L.J., Kim, F., Huang, J.X., 2009. J. Am. Chem. Soc. 131, 1043–1049.
Dong, H.F., Gao, W.C., Yan, F., Ji, H.X., Ju, H.X., 2010. Anal. Chem. 82, 5511–5517.
Georgopoulos, P.G., Roy, A., Yonone-Lioy, M.J., Opiekun, R.E., Lioy, P.J., 2001. J. Toxicol. Environ. Health, B 4, 341–394.
Guo, H.-L., Wang, X.-F., Qian, Q.-Y., Wang, F.-B., Xia, X.-H., 2009. ACS Nano 3, 2653–2659.
He, S.J., Song, B., Li, D., Zhu, C.F., Qi, W.P., Wen, Y.Q., Wang, L.H., Song, S.P., Fang, H.P., Fan, C.H., 2010. Adv. Funct. Mater. 20, 453–459.
Jeng, E.S., Moll, A.E., Roy, A.C., Gastala, J.B., Strano, M.S., 2006. Nano Lett. 6, 371–375.
Jennings, T.L., Singh, M.P., Strouse, G.F., 2006. J. Am. Chem. Soc. 128, 5462–5467.
Kata, E., Willner, I., 2004. Angew. Chem. Int. Ed. 43, 6042–6108.
Kim, C.K., Kalluru, R.R., Singh, J.P., Fortner, A., Griffin, J., Darbha, G.K., Ray, P.C., 2006. Nanotechnology 17, 3085–3093.
Kim, J., Cote, L.J., Kim, F., Huang, J.X., 2010. J. Am. Chem. Soc. 132, 260–267.
Kong, D.-M., Ma, Y.-E., Guo, J.-H., Yang, W., Shen, H.-X., 2009. Anal. Chem. 81, 2678–2684.
Lee, J.H., Wang, Z.D., Liu, J.W., Lu, Y., 2008. J. Am. Chem. Soc. 130, 14217–14226.
Li, J., Lu, Y., 2000. J. Am. Chem. Soc. 122, 10466–10467.
Li, J., Zheng, W.C., Kwon, A.H., Lu, Y., 2000. Nucleic Acids Res. 28, 481–488.
Li, X.L., Zhang, G.Y., Bai, X.D., Sun, X.M., Wang, X.R., Wang, E.G., Dai, H.J., 2008. Nat. Nanotechnol. 3, 538–542.
Li, T., Dong, S.J., Wang, E.K., 2009. Anal. Chem. 81, 2144–2149.
Li, T., Dong, S.J., Wang, E.K., 2010a. J. Am. Chem. Soc. 132, 13156–13157.
Li, T., Wang, E.K., Dong, S.J., 2010b. Anal. Chem. 82, 7576–7580.
Li, T., Wang, E.K., Dong, S.J., 2010c. Anal. Chem. 82, 1515–1520.
Liu, J.W., Lu, Y., 2003. Anal. Chem. 75, 6666–6672.
Liu, J.W., Lu, Y., 2005. J. Am. Chem. Soc. 127, 12677–12683.
Liu, J.W., Lu, Y., 2007a. J. Am. Chem. Soc. 129, 9838–9839.
Liu, J.W., Lu, Y., 2007b. Chem. Commun., 4872–4874.
Liu, J.W., Lu, Y., 2007c. Angew. Chem. Int. Ed. 46, 7587–7759.
Liu, Z., Robinson, J.T., Sun, X.M., Dai, H.J., 2008. J. Am. Chem. Soc. 130, 10876–10877.
Liu, Y., Wang, Y.X., Jin, J.Y., Wang, H., Yang, R.H., Tan, W.H., 2009. Chem. Commun., 665–667.
Liu, M., Zhao, H.M., Quan, X., Chen, S., Yu, H.T., 2010a. Chem. Commun. 46, 1144–1146.
Liu, M., Zhao, H.M., Quan, X., Chen, S., Fan, X.F., 2010b. Chem. Commun. 46, 7909–7911.
Lu, C.H., Yang, H.H., Zhu, C.L., Chen, X., Chen, G.N., 2009. Angew. Chem. Int. Ed. 48, 4785–4787.
Mei, S.H.J., Liu, Z., Brennan, J.D., Li, Y.F., 2003. J. Am. Chem. Soc. 125, 412–420.
Moshe, M., Elbaz, J., Willner, I., 2009. Nano Lett. 9, 1196–1200.
Qin, H.X., Ren, J.T., Wang, J.H., Wang, E.K., 2010a. Chem. Commun. 46, 7385–7387.
Qin, H.X., Ren, J.T., Wang, J.H., Luedtke, N.W., Wang, E.K., 2010b. Anal. Chem. 82, 8356–8360.
Saini, S., Srinivas, G., Bagchi, B., 2009. J. Phys. Chem. B 113, 1817–1832.
Shang, L., Dong, S.J., 2008. J. Mater. Chem. 18, 4636–4640.
Singh, M.P., Strouse, G.F., 2010. J. Am. Chem. Soc. 132, 9383–9391.
Song, Y.J., Qu, K.G., Xu, C., Ren, J.S., Qu, X.G., 2010. Chem. Commun. 46, 6572–6574.
Tang, Z.W., Wu, H., Cort, J.R., Buchko, G.W., Zhang, Y.Y., Shao, Y.Y., Aksay, I.A., Liu, J., Lin, Y.H., 2010. Small 6, 1205–1209.
Vulpe, C., Levinson, B., Whitney, S., Packman, S., Gitschier, J., 1993. Nat. Genet. 3, 7–13.
Waggoner, D.J., Bartnikas, T.B., Gitlin, J.D., 1999. Neurobiol. Dis. 6, 221–230.
Wang, Z.D., Lee, J.H., Lu, Y., 2008. Adv. Mater. 20, 3263–3267.
Wang, H., Yang, R.H., Yang, L., Tan, W.H., 2009. ACS Nano 3, 2451–2460.
Wen, Z.-C., Yang, R., He, H., Jiang, Y.-B., 2006. Chem. Commun., 106–108.
Wu, C., Oo, M.K.K., Fan, X.D., 2010. ACS Nano 4, 5897–5904.
Xiang, Y., Yong, A.J., Lu, Y., 2009. J. Am. Chem. Soc. 131, 15352–15357.
Xiang, Y., Wang, Z.D., Xing, H., Wong, N.Y., Lu, Y., 2010. Anal. Chem. 82, 4122–4129.
Xu, W.C., Lu, Y., 2010. Anal. Chem. 82, 574–578.
Xu, X.Y., Daniel, W.L., Wei, W., Mirkin, C.A., 2010. Small 6, 623–626.
Yang, R.H., Tang, Z.W., Yan, J.L., Kang, H.Z., Kim, Y., Zhu, Z., Tan, W.H., 2008a. Anal. Chem. 80, 7408–7413.
Yang, R.H., Jin, J.Y., Chen, Y., Shao, N., Kang, H.Z., Xiao, Z.Y., Tang, Z.W., Wu, Y.R., Zhu, Z., Tan, W.H., 2008b. J. Am. Chem. Soc. 130, 8351–8358.
Yin, B.-C., Ye, B.-C., Tan, W.H., Wang, H., Xie, C.-C., 2009. J. Am. Chem. Soc. 131, 14624–14625.
Yun, C.S., Javier, A., Jennings, T., Fisher, M., Hira, S., Peterson, S., Hopkins, B., Reich, N.O., Strouse, G.F., 2005. J. Am. Chem. Soc. 127, 3115–3119.
Zeng, L., Miller, E.M., Pralle, A., Isacoff, E.Y., Chang, C.J., 2006. J. Am. Chem. Soc. 128, 10–11.
Zhang, L.B., Li, T., Li, B.L., Li, J., Wang, E.K., 2010a. Chem. Commun. 46, 1476–1478.
Zhang, X.-B., Wang, Z.D., Xing, H., Xiang, Y., Lu, Y., 2010b. Anal. Chem. 82, 5005–5011.
Zhou, Y., Wang, S.X., Zhang, K., Jian, X.Y., 2008. Angew. Chem. Int. Ed. 47, 7454–7456.
Zhou, Y., Bao, Q.L., Tang, L.A.L., Zhong, Y.L., Loh, K.P., 2009. Chem. Mater. 21, 2950–2956.
Zietz, B.P., Dieter, H.H., Lakomek, M., Schneider, H., Kebler-Gaedtke, B., Dunkelberg, H., 2003. Sci. Total Environ. 302, 127–144.